Experimental Studies on Characteristics of Fire Whirl in a Vertical Shaft

Short title: Characteristics of Fire Whirl in a Vertical Shaft

Zheming GAO, Shusheng LI and Ye GAO

College of Aerospace and Civil Engineering

Harbin Engineering University

Harbin, Heilongjiang, China

Wan Ki CHOW*

Research Centre for Fire Engineering

Department of Building Services Engineering

The Hong Kong Polytechnic University

Hong Kong, China

*Corresponding author:

Fax: (852) 2765 7198; Tel: (852) 2766 5843

Email: beelize@polyu.edu.hk; bewkchow@polyu.edu.hk

Postal address: Department of Building Services Engineering, The Hong Kong Polytechnic University, Hunghom, Kowloon, Hong Kong

Experimental Studies on Characteristics of Fire Whirl in a Vertical Shaft

Abstract

An internal fire whirl can be generated readily in a tall shaft model with appropriate gap width at one corner. Experimental study was carried out to investigate the relationship between the characteristics of an IFW and the corner gap width in a 9-m tall vertical shaft model. The vertical shaft had a 2.1 m by 2.1 m square section with gasoline pool fire of different diameters burning inside. The gap width was varied to investigate its impact on fire whirl characteristics, such as flame development, swirling intensity, flame height, flame temperature and heat release rate of the gasoline pool fire. Vigorous flame swirling motions were generated when the ratio of the gap width to the shaft section perimeter was within the range 0.16 to 0.21. From the flame streamline angle, it was observed that the swirling component was much stronger than buoyancy component near the bottom of burning region. The swirling component decreased and became roughly the same as buoyancy near the middle. Finally, it diminished to being much weaker than buoyancy near the top of the fire. These observations suggest that the Froude number Fr decreased from a large number to 1, and then continued to decrease to 0.

1.   Introduction

Fire whirls above burning objects, compared with non-swirling fires, have higher temperatures, flame heights, burning rates and flame intensity, leading to much more hazardous scenarios. A fire whirl can also be generated indoor and is referred to as an Internal Fire Whirl (IFW) in this paper to distinguish it from external fire whirl. IFW was not regarded as an important phenomenon to consider in fire safety before, because an IFW can only be generated under appropriate ventilation conditions to start swirling. However, in new tall buildings with green features such as solar chimney[1,2], an IFW can be generated readily[3,4] in the vertical shafts. If these shafts have a corner gap of appropriate size, an IFW will be generated even when a small fire occurs. Therefore, the hazardous consequence of having the IFW scenario should be included in hazard assessment.

Early studies related to experimental IFW inside a modeling facility include the pioneer work in the Southern Forest Fire Laboratory in Macon, Georgia,[5,6] and the fire whirl generated from an acetone pool placed at the centre of a rotating cylindrical screen by Emmons and associates.[7-9] Vorticities pertaining to fire whirl were presented by Morton.[10] IFW and the associated building fluid dynamics were investigated by Meroney.[11] Fire vortices can form only where vorticity of appropriate strength coupled with an approximately vertical orientation is first generated, and then amplified by the ambient air as reported in the literature[12-16].

Small-scale experiments are commonly used to study the effect of circulation on the formation of fire whirl. Lei et al.[17,18] quantitatively explored the characteristics of flame instability and obtained the relationships between heat release rate, temperature, velocity and circulation in IFWs by a four-wall fixed-frame experiment facility. Satoh and Yang[3,4,19] generated fire whirl in a vertical shaft with corner gap. The results show that the gap size is an important factor in determining flame swirl intensity. A small-scale IFW was produced[14] in a fixed-frame type facility with two-split cylinders[17]. The flow fields of the fire whirl at different gap sizes of the two-split cylinders were measured using stereo particle image velocimetry.

A method was proposed by Zhou[20] for analysis and prediction of spontaneous IFW due to irregularly or randomly distributed flame sources, by defining an equivalent gap fraction and providing an adapted criterion. Based on the experimental results obtained in a real-sized experimental facility, Dobashi and Okura[21] proposed two probable mechanisms for the increase of fire whirl height. The first is attributed to more heat transfer to the fuel burning surface, which enhances the vaporization rate. In the second mechanism, the increase in flame height is attributed to the interaction between swirling flow and flame. Increase in temperature due to the increased entrainment of air, which increases the combustion rate is emphasized to be an important factor. In summary, flame with swirl would lead to higher combustion surface temperature, better air and fuel mixture and easier fuel vaporization.

A small-scale vertical shaft model (34 cm × 35 cm × 145 cm) was constructed by Chow and Han[22,23] to study IFW thoroughly. Compared with free burning, the presence of a vertical gap of appropriate width and height at the side wall would lead to IFW[22]. Flame height would be stretched to several times the value for free burning. Additionally, it was found in the scale model by Chow and Han[22,23] that IFW can only be generated when the gap width lies within a certain range (1.55 cm to 3.6 cm in this model of 145 cm in height). A linear correlation between flame height and mass fuel burning rate can be determined for different liquid

fuels[23].

Full-scale experiments have been performed for further investigation of IFW formation mechanism. Tall vertical shafts (9 m, 12 m and 15 m in height) with a single corner gap were constructed by Chow and associates[24-27] to study the characteristics of IFW, with results showing that burning rate and flame height varied with gap width. The temperature and burning rate of free pool fire and fire whirl were compared and CFD was used to predict the tangential velocity of fire whirl[24]. The evolution of an IFW can be divided into five stages[25]: the initial stage, flame rising-up stage, stable flame, whirling stage and decay stage. Based on the flame height correlations for free burning pool fires, the fuel consumption rate of the pool fire in the shaft was estimated. Correlations of the whirling flame height with fuel mass and other key parameters were then derived. Furthermore, the generated IFW can be divided into three zones[26]. Zone I is at the lower part with the flame rotating violently. Zone II is in the middle part with a slower swirling rate. The upper part zone III has no flame rotation. From the experimental observations[27] on flame swirling for different gap widths coupled with three assumptions on variation of air entrainment velocity with height, an expression of the flame height was derived for the IFW using one set of compiled experimental data.

The main differences between this paper and previous studies by the same group[22-27] are:

- The generation process of the IFW was not studied in these previous studies, which only focused on factors affecting the height of the swirling flame.
- A more rigorous quantitative analysis of the relationship between gap width and flame height is presented in this study.
- The fuel evaporation rate of the fire whirl is determined in this study.
- This study provides a flame height comparison between non-whirling fire and fire whirl.
- The Froude number Fr is taken as the characteristic number to describe the fire swirling intensity for the first time.

As a summary, previous works[22-27] studied the generation mechanism of IFW and the relations between circulation, temperature and flame height. Detailed quantitative analysis about the relationships between gap width and flame height or swirl intensity has not yet been studied, though a correlation of flame height with gap width was reported very recently.[21] In the present study, the flame height, burning duration and temperature of different oil pools under different gap widths are compared. The range of gap width generating IFW and the conditions giving the strongest IFW are proposed. The effect of liquid fuel pools with different diameters on the generation of fire whirl under a certain gap width is discussed. The measurements from these tests are used to calculate the fire whirl parameters, flame height and vaporization rate. Moreover, the Froude number Fr is identified as the parameter to describe the swirl intensity of fire whirl.

2. Experimental Studies

A 9-m tall vertical shaft of square section 2.1 m x 2.1 m was constructed[26,27] as shown in Fig. 1(a). A corner gap of adjustable width was incorporated to control the air entrainment from outside the shaft. Two glass panes were installed on the front wall for visualization. The rest of the walls were made of 0.1 cm thick steel plate. The top of shaft was fully opened. An electronic scale under the pool was used to record the fuel loss rate.

Two sets of experiments were carried out in this study (see Table 1):

- Experiment 1:

  A 0.46-m diameter pool fire with 3 litres of gasoline was placed at the centre of the bottom. A total of 8 tests, labeled SW 1 to SW 8, corresponding to gap width of 0.013 m, 0.055 m, 0.11 m, 0.22 m, 0.33 m, 0.44 m, 0.66 m, and 0.88 m respectively were conducted.

  Gas temperature measurement points are shown in Fig. 1(b). Two vertical thermocouple trees in the middle (M) and at the corner (C) were installed. The thermocouples in tree M and C were positioned at regular intervals of 0.9 m, M1 and C1 were 0.9 m above the ground.

- Experiment 2:

  The gap width was fixed at 0.33 m. Three tests SW-S, SW-M ,SW-L corresponding to 0.2 m, 0.26 m, 0.46 m in fuel diameter were conducted. The oil depth was set at 4 cm, giving 1.25 L, 2.12 L, 6.65 L of gasoline in SW-S, SW-M, SW-L.

  Gas temperature measurement points are shown in Fig. 1(b). A thermocouple tree T was put at the middle position as M. The lower 10 thermocouples in tree T were positioned at regular intervals of 10 cm, and the upper 10 with regular intervals of 15 cm. T1 was 10 cm above the ground.

To ensure repeatability of the experimental study, transient central vertical temperatures at T1, T6, T12 and T22 for test SW-L were measured three times, with results shown in Fig. 2. The temperature curves rose up to a maximum level and remained nearly constant for some time and then dropped rapidly when all fuel was burnt out. During the steady burning period, gas temperatures fluctuated within a small range. Results of the three replicate tests agreed well at the growth stage and steady burning stage. Only small discrepancy existed at the decay stage. As the present study was mainly focused on the steady burning stage, the results indicated good repeatability. Thus only one test was conducted for each condition.

The measured flame shape, burning duration and temperature distribution were then used to study the effect of the corner gap width on the IFW development.

As reported before,[22-27] once an IFW is generated under appropriate vertical shaft ventilation, the fire parameters such as air temperature, flame height, burning rate and burning duration all have good repeatability. Repeating test SW-L on the bigger scale experiment with a larger IFW would allow easier observation of the whole process from generation to extinction. Tests were repeated three times to illustrate that an IFW can be generated inside the vertical shaft model with a single corner gap without an open roof.

3.   Results

In Experiment 1, the results and the photographs for the tests are summarized in Table 2. Although the pool fire diameter and the amount of fuel were kept unchanged, the fire whirl intensity varied substantially with the change of gap width d (in m). From the photographs in

Table 2 and the video, the following was observed:

- At d of 0.013 m, no clear fire whirl structure was observed.
- At 0.055 m, flame was elongated, but the rotating motion was not significant.
- At 0.11 m, an unstable fire whirl was generated with the flame moving up and down.
- At 0.22 m, fire swirling occurred and the flame fluctuated slightly.
- At 0.33 m and 0.44 m, a stable IFW was generated with little fluctuation.
- At 0.66 m, an IFW still existed, but with flame fluctuation.
- At 0.88 m, an IFW was generated only intermittently.

Air entrained into the shaft from the corner gap plays two roles in generating an IFW:

- Firstly, a torque about the fire axis was provided by the incoming air to generate the whirling motion.
- Secondly, the incoming air provided more oxygen for supporting a higher combustion rate of the swirling flame.

Both of these functions depend on d. A narrower gap favors higher entrained air velocity while a wider gap favors more air entrainment. For both these roles to be favorable factors in generating and sustaining the IFW, d must lie within a certain range under the experimental conditions in the present study. When the gap width is outside this range, either the torque is inadequate to generate or maintain the whirling motion (gap too wide) or the amount of entrained air is not sufficient to support the high combustion rate in IFW (gap too narrow).

In addition, it was observed that the flame height grew with the increase of rotating intensity. The maximum flame height reached a value which was about 2.5 times the non-swirling flame height (Table 2). The burning duration of a fire whirl was also reduced to about one half of the burning time of a free burning fire.

To understand the quantitative effect of the gap width on flame swirling, a dimensionless gap width d^* is defined.

$$d^* = \frac{d}{L} \tag{1}$$

The effect of gap width on transient gas temperature is shown in Fig. 3. The centerline temperature decreased quickly along thermocouple tree M. The transient gas temperatures of M1 in all 8 cases of different d values are plotted in Fig. 3(b). Gas temperature fluctuated for some cases when the generated IFW was not stable. Cases with higher temperature were those tests that generated a stable IFW with shorter burning time. The average temperature at M1 was plotted against d^* in Fig. 3(c). The highest temperature was reached when d^* was within the range 0.16 to 0.21. For $d^*<0.16$, as well as for $d^*>0.21$, the flame temperature decreased.

The average temperature of thermocouple tree C for Experiment 1 is shown in Fig. 4. The corner temperature distribution did not show significant difference between fire whirl scenario and normal pool fire scenario.

The average centerline gas temperatures at thermocouple tree T in Experiment 2 are shown in

Fig. 5. For $d*$=0.16, larger fuel diameter gave larger heat release rate. Therefore increased temperature and buoyancy resulted in higher flame. The temperature of SW-L near pool surface was lower than those of the others. It is because the fuel vaporization removed heat from the pool surface. Within the three fuel pool experiments, the luminous region of larger fuel pool was longer but the intermittent region length was similar. The highest points of flame were corresponding to the descending portion of plume region

According to the data record of the electronic scale, the gasoline mass per unit area in the three cases (SW-S, SW-M, SW-L) are shown as a function of time in Fig. 6. The mass loss rate per unit area (m_∞) as given by the slope is similar for each experiment. The stable generation of fire whirl greatly increases the value of this parameter. Comparing with pool fire research[28-32] in Table 3, $m \approx 0.096 kg/m^2 \cdot s$ is obviously larger than the values in these references.

A fire whirl can be split into an axial upward motion and a tangential motion, as shown schematically in Fig. 7. It swirls strongly at the bottom with a large tangential velocity. The upward air-flow velocity of a fire whirl increases first and then decreases with height. The tangential velocity comes from the inhalation of air from the gap and the upward velocity is caused by buoyancy.

4. Analysis of vaporization rate

Buoyancy induced by the density difference of hot gases would become the driving force to entrain cool air flowing to the shaft model through the gap. Limiting the air motion by the shaft wall would give rotating flow. These two forces will become driving force of the IFW as reported before[e.g. 11]. Assuming that the velocity of the upward air flow at the root of the flame is 0, and all the buoyancy is converted to the rotating force, the flame is similar to a rotating cylinder of fluid, and the tangential velocity v_θ has the maximum value $v_{\theta max}$. In the cylindrical coordinate system, the conservation of momentum equation Eq. (2) exists on any constant height surface. The density of ambient air is $\rho_\infty = 1.21 kg/m^3$. According to the temperature data measured in the experiment, taking 1000K as the flame root temperature, the gasoline vapour density at this temperature is $\rho_a = 0.18 kg/m^3$. Let r_0 be the pool radius (in m). In cylindrical coordinate, the momentum equation at any contour plane is

$$\frac{v_\theta^2}{r} = \frac{1}{\rho}\frac{dp}{dr} \tag{2}$$

Integrating both sides of the equation (2):

$$\int_0^{r_0} \frac{v_\theta^2}{r} dr = \int_0^{r_0} \frac{1}{\rho}\frac{dp}{dr} dr \tag{3}$$

Assuming $v_\theta|_{r=0} = 0$,

$$v_\theta = v_{\theta\,\text{max}} = \sqrt{\frac{2r_0(\rho_g - \rho_a)\,\text{g}}{\rho_g}} \tag{4}$$

For SW-S, SW-M and SW-L, $v_{\theta\,\text{max}}$ =3.33m/s, 3.8m/s and 5.37m/s respectively.

The heat transmitted to the gasoline surface is composed of three modes: heat conduction, convection and radiation. Heat conduction is small, usually negligible. Convection and radiation can be deduced from the following formulas.

The heat transfer surface is taken to be at the gasoline level. Because of the heat absorption of gasoline, heat transfer and surface temperature will not continue to rise. Therefore, the gasoline surface would have temperature equal to the boiling point of gasoline $T_w = 493K$. These modifications are based on the literature[33,34]. The thermal conductivity of gasoline λ_1 at $T_w = 493K$ is 0.0253 Wm^{-1}K^{-1}. The kinetic viscosity $v_1 = 1.37 \times 10^{-4} m^2 s^{-1}$. Stefan-Boltzmann constant $\sigma = 5.67 \times 10^{-8}$ Wm^{-2}K^{-4}. L is the characteristic length (in m), taking Pr = 0.7 and emissivity $\varepsilon = 0.85$.

The Reynolds number Re is given by

$$\text{Re} = \frac{v_{\theta\,\text{max}} L}{v_1} = \frac{3.33 \times 0.2}{1.37 \times 10^{-4}} = 4865.2 < 5000 \tag{5}$$

The Nusselt Number Nu[35] is given by

$$Nu = 0.332\,\text{Re}^{\frac{1}{2}}\,\text{Pr}^{\frac{1}{3}} = 20.56 \tag{6}$$

$$h_{1conv} = Nu\frac{\lambda_1}{L} = \frac{20.56 \times 0.0253}{0.2} = 2.6\,\text{Wm}^{-2}K^{-1} \tag{7}$$

$$h_{1rad} = \frac{\varepsilon\sigma(\text{T}_f^4 - \text{T}_w^4)}{T_f - T_w} = \frac{0.85 \times 5.67 \times 10^{-8} \times (1000^4 - 493^4)}{(1000\text{-}493)} = 89.44\,\text{Wm}^{-2}K^{-1} \tag{8}$$

As seen above, most of the heat transferred to the gasoline surface comes from flame radiation. That is to say convection itself is not the key factor to enhance the heat release rate and height of flame, but the increase of air inflow caused by convection, resulting in stronger chemical reaction. The following Eq. (9) can be used to evaluate the total transfer coefficient for the inner surface,

$$h_1^{\frac{4}{3}} = h_{1conv}^{\frac{4}{3}} + h_1^{\frac{1}{3}}h_{1rad} \tag{9}$$

Thus, the heat transfer coefficient is given by

$$h_1 = 90.2\,Wm^{-2}K^{-1} \tag{10}$$

The heat transfer rate from flame to gasoline surface is given by

$$q_1 = h_1 A_B (T_f - T_w) = 90.2 \times 3.14 \times 0.1^2 \times (1000 - 493) = 1435.97W \tag{11}$$

When the combustion is stable, the temperature of gasoline and fuel tank are considered as the same. The fuel tank is made of steel, quite an amount of heat transfers from the fuel tank to air by heat convection and radiation. The ambient air temperature $T_\infty = 293K$. Thermal conductivity of air λ_2 at $T_\infty = 293K$ is 0.0657 Wm⁻¹K⁻¹.

The area of fuel tank bottom is given by

$$A_B = \pi r^2 = 0.0314m^2 \tag{12}$$

The volume expansion coefficient is given by

$$a = \frac{1}{T_w - T_\infty} = \frac{1}{493 - 293} = 0.005K^{-1} \tag{13}$$

Then, the Grashof Number Gr^{36} is calculated by the following formula

$$Gr = \frac{gaL_B{}^3(T_w - T_\infty)}{v_2{}^2} = \frac{9.8 \times 0.005 \times 0.2^3 \times (493 - 293)}{(3.25 \times 10^{-5})^2} = 7.42 \times 10^7 < 10^9 \tag{14}$$

Laminar convection heat transfer can be assumed when Gr<10⁹ and the Nusselt Number Nu under this condition is given by

$$Nu = 0.48(Gr \cdot \mathrm{Pr})^{\frac{1}{4}} = 40.8 \tag{15}$$

The heat transfer coefficient is given by

$$h_{2Bconv} = Nu \frac{\lambda_2}{L_B} = 37.5 \times \frac{0.0657}{0.2} = 13.4 Wm^{-2}K^{-1} \tag{16}$$

The heat release rate from fuel tank bottom to air is given by

$$q_{Bconv} = h_{2Bconv} A_B (T_w - T_\infty) = 13.4 \times 0.0314 \times (493 - 293) = 84.1W \tag{17}$$

For the fuel tank side wall, the area is given by

$$A_S = \pi DH = 3.14 \times 0.2 \times 0.04 = 0.02512m^2 \tag{18}$$

Similarly for the fuel tank bottom,

$$Gr = \frac{gaL_S{}^3(T_w - T_f)}{v_2{}^2} = \frac{9.8 \times 2.18 \times 10^{-3} \times 0.04^3 \times (493 - 293)}{(3.25 \times 10^{-5})^2} = 5.94 \times 10^5 < 10^9 \tag{19}$$

9

$$Nu = 0.48(Gr \cdot \mathrm{Pr})^{\frac{1}{4}} = 12.2 \tag{20}$$

$$h_{2Sconv} = Nu \frac{\lambda_2}{L_S} = 12.2 \times \frac{0.0657}{0.04} = 20 Wm^{-2} K^{-1} \tag{21}$$

$$q_{Sconv} = h_{2Sconv} A_S (T_w - T_\infty) = 20 \times 0.02512 \times (493 - 293) = 100.6\,\mathrm{W} \tag{22}$$

L_S is the fuel tank side wall length (0.04 m) which can transfer heat to ambient air. The radiation heat release rate from both the fuel tank bottom and side wall can be calculated from the following equation

$$q_{2rad} = \varepsilon \sigma (A_B + A_S)(T_w^{\,4} - T_\infty^{\,4}) = 140.8\,\mathrm{W} \tag{23}$$

Thus, the total heat release rate from the fuel tank to air is

$$q_2 = q_{2Sconv} + q_{2Bconv} + q_{2rad} = 325.5W \tag{24}$$

The heat release rate resulting in gasoline vaporization therefore can be expressed as

$$\Delta q = q_1 - q_2 = 1110.5W \tag{25}$$

The specific vaporization heat of gasoline $\Delta h_v = 3.5 \times 10^5 J / \mathrm{kg}$, thus the mass flux is

$$m_{SW-S}{}' = \frac{\Delta q}{\Delta h_v A} = \frac{1110.5}{3.5 \times 10^5 \times 0.0314} = 0.101 kgm^{-2}s^{-1} \tag{26}$$

Similarly, using the above equations, the mass flux of SW-M and SW-L is $m_{SW-M}{}' = 0.101 kgm^{-2}s^{-1}$ and $m_{SW-L}{}' = 0.104 kgm^{-2}s^{-1}$ respectively.

5. Flame Height Estimate

Heat release rate and flame height are the two key parameters of a fire whirl. The correlations of these two parameters with the gap width are investigated in the present study. The measured flame height L_f is plotted against the dimensionless gap width $d*$ in Fig. 8, together with a fitting curve (shown in black).

When $0.1 < d* < 0.4$, the equation relating the fitted flame height L_{ff} to the dimensionless gap width $d*$ is given by

$$L_{ff} = 200 d^{*3} - 155 d^{*2} + 34.5 d^* + 1.5 \tag{27}$$

Note that $d* > 0.1$ marks the onset of swirling and the equation applies to a fire whirl. IFW cannot form when $d* > 0.43$.

Normalizing with the maximum flame height $L_{ff\,max}$ gives:

$$L_{ff} / L_{ff\,max} = 55.6d^{*3} - 43.1d^{*2} + 9.6d^{*} + 0.42 \tag{28}$$

The total heat release rate of the swirling flame can be deduced from the combustion time, the specific heat of combustion for gasoline ΔH_c is 43700kJ/kg, and the fuel mass loss in Table. 4. The gasoline combustion rate coefficient C is assumed to be 0.8. Thus,

$$Q = \frac{M}{\Delta H \cdot t} \tag{29}$$

Q and other parameters in different cases are shown in Table 4.

The flame height L_f (in m) is a function of heat release rate q^* and fire source diameter D_f (in m).

$$L_f = 3.3q^{*2/5}D_f \tag{30}$$

$$q^* = \frac{Q}{\rho_0 T_0 c_p \sqrt{gD_f} D_f^2} \tag{31}$$

Moreover, McCaffrey[37], Heskestad[38], Hasemi and Tokunaga[39] also proposed equations for flame height. In general L_f / D_f is proportional to $q^{*\,2/5}$.

Assuming that for an IFW, L_f / D_f is also proportional to $q^{*\,2/5}$ when $0.16 < d* < 0.21$, then the flame height equation for a fire whirl can be modified to:

$$L_f = Xq^{*2/5}D_f \tag{32}$$

where X is a coefficient characteristic of the fire whirl.

Putting $\rho_0 = 1.293$ kg/m^3, $T_0 = 308.15$ K, $c_P = 1.004$ kJ/kg $\cdot$ K, $g = 9.8$ m/s^2 and the heat release rate of the three experiments and the average flame height of stable phase in Eqs. (6) and (7), the value of the coefficient X can be calculated, with results given in Table 4. The average value of X is 5.07, and the equation of an internal fire whirl height is given by:

$$L_f = 5.07q^{*2/5}D_f \tag{33}$$

In Eq. (8) the dimensionless gap width ranges from 0.16 to 0.21, where the flame height is the largest. To combine the fire source diameter D_f and dimensionless gap width d^*, multiplication of Eq. (8) by Eq. (3) gives an empirical formula for the flame height of an IFW:

$$L_f = 5.07 \frac{L_{ff}}{L_{ff\,max}} q^{*\frac{2}{5}} D_f \tag{34}$$

As $5.07*L_{ff}/L_{ff\,max}$ reflects the effect of circulation Γ, the flame height is related to Γ or V_θ. The fitted results for Experiment 1 and Experiment 2 are compared with measurements as shown in Fig. 8.

6.   Froude Number Modelling

The Froude number Fr (defined by Eq. (10) below) in a fire whirl changes with height.

$$Fr = \sqrt{V^2/gL} \tag{35}$$

In the experiment, three states of Fr can be identified as shown in Fig. 9. The picture is taken from the SW-L. In order to be able to see the flame flow texture more clearly, the flame is shown in blue color. The streamline at the bottom of flame was almost parallel to the ground, which means that circulatory inertia force was much stronger than buoyancy, giving $Fr \gg 1$ under this situation. At the middle and lower part of the swirling flame, the angle between the streamline and the ground was about 45°. The circulatory inertia force and buoyancy were roughly the same, giving $Fr \approx 1$. Buoyancy dominated over circulatory inertia force in the upper half of flame and the streamlines were basically perpendicular to the ground, and in this case $Fr \ll 1$, that is $Fr \approx 0$.

The relationship between gap width and flame height shows that the Froude number, which is the ratio of baroclinic force to buoyancy, would significantly affect the flame height. The longer the region for which $Fr > 1$, the taller the flame will be. The temperature at the bottom of swirling flame where $Fr \gg 1$ determines the mass of air sucked into the shaft and hence the combustion efficiency or heat release rate. The flame height is affected mostly by the circulatory inertia force. The value and variation of circulatory inertia force are dominated by the difference in temperature and density of flame compared with the external environment.

7.   Conclusions

A 9-m height square vertical shaft with a circular pool fire at the centre of the shaft bottom was employed for the generation of IFW. IFW has a totally different structure compared with the normal pool fire in open space. The uprising whirling flow not only maintains an axial velocity, but also possesses tangential velocity. The streamlines form an upward spiral. Besides, the swirling flame is longer, brighter, higher in temperature and has a sharper outline.

By adjusting the gap width, different swirling intensity could be observed. The flame height reached the highest value and the swirl was the strongest when gap width was within a critical range. In addition, the consumption of gasoline fuel was faster. Internal fire whirl formation is not favored when the gap is either too narrow or too wide. When $0.16 < d^* < 0.21$, the most intensive fire whirl was generated; the flame temperature and flame height reached the maximum value. For gap width within this range the large difference in temperature and hence in density between the flame and external environment would suck in air at a higher rate. Increased air supply would give more complete chemical reaction, higher heat release rate, and higher temperature. When d^* is outside the above range, flame rotation intensity is relatively weak or even absent, resulting in lower flame temperature and lower flame height.

The experimental results show that the gap width of a vertical shaft is the key factor in determining flame height and swirling intensity. In conclusion, particular attentions should be paid to the gap width of vertical shaft or similar structures to avoid the generation of internal fire whirl.

Declaration of Conflicts of Interest

The authors declare that there is no conflict of interest regarding the publication of this article.

Funding

Nomenclature

A_B	Fuel tank bottom area, m^2
A_S	Area of side wall, m^2
a	Volume expansion coefficient, K^{-1}
c_p	Air specific heat capacity, kJ/kg·K
d^*	Dimensionless gap width
d	Gap width, m
D_f	Pool diameter, m
Fr	Froude number.
g	Gravitational acceleration, m/s^2.
Gr	Grashof Number
H	Gasoline depth, m
h	Heat transfer coefficient, Wm^{-2}K^{-1}
L	Characteristic length, m
L_f	Flame height, m
L_{ff}	Fitted flame height, m
$L_{ff\,max}$	Maximum flame height, m
m	Heat flux, kg/m^2·s
m'	Calculated mass flux, kg/m^2·s
Nu	Nusselt Number
P	Local pressure, Pa
P_∞	Atmospheric pressure, Pa
Pr	Prandtl Number
q	Heat release rate, kw
q^*	Heat release rate coefficient
Q	Heat release rate of flame, kw
r	Pool radius, m
Re	Reynolds number
T_w	Fuel surface temperature, K
T_f	Flame temperature, K
T_∞	Ambient air temperature, K
V_θ	Tangential velocity, m/s
X	Coefficient characteristic of the fire whirl

Greek letters

Δq	The heat release rate that causes vaporization, W
ΔH_c	The heat of combustion, kJ/kg
β	Mean-beam-length corrector
ρ_a	Gasoline vapour density, kg/m^3
ρ_∞	Ambient air density, kg/m^3,
λ	Thermal conductivity, Wm^{-1}K^{-1}
v_1	Kinetic viscosity of gasoline, m^{2}s^{-1}
σ	Stefan-Boltzmann constant, Wm^{-2}K^{-4}
ε	emissivity

Subscripts

1	From flame to fuel surface
2	From fuel tank to ambient air
B	From fuel tank bottom to ambient air
S	From fuel tank side wall to ambient air
Conv	Convective heat transfer
rad	Radiative heat transfer

References

[1]   Chow CL, Chow WK. Initial buoyancy reduction in exhausting smoke with solar chimney design. *J. Heat Transfer – Transactions of the ASME*, 2010; 132(1): 014502-1 to 014502-3, Article No. 014502.

[2]   Chow WK. Performance-based approach to determining fire safety provisions for buildings in the Asia-Oceania regions. *Build. Environ. - Fifty Year Anniversary of Building and Environment*, 2015; 91: 127-137.

[3]   Satoh K, Yang KT. Experiments and numerical simulations of swirling fires due to 2×2 flames in a shaft with single corner gap. *Proc. ASME, Heat Transfer Division*, 1998; 361(2): 49-56

[4]   Satoh K, Yang KT. Measurements of fire whirls from a single flame in a vertical square shaft with symmetrical corner gaps. *Proc. ASME, Heat Transfer Division*, 1999; 364(4): 167-173

[5]   Byram GM, Martin RE. Fire whirlwinds in the laboratory. *Fire Control Notes*, 1962; 23(1): 13-17

[6]   Byram GM, Martin RE. The modeling of fire whirl winds. *Forest Science*, 1970; 16(4): 386-399.

[7]   Emmons HW. Fundamental problems of the free burning fire. *Tenth Sym. (Int.) Combust.*, The Combustion Institute, 1965, pp. 951-964

[8]   Ying SJ. The fire whirl. PhD thesis, Harvard University, 1965.

[9]   Emmons HW, Ying SJ. The fire whirl. *Eleventh Sym. (Int.) Combust.*, The Combustion Institute, Pittsburgh, Pennsylvanina, USA, 1967, pp. 475-488.

[10]   Morton BR. The physics of fire whirls. *Fire Research Abstracts and Reviews*, 1970; 12(1): 1-19

[11]   Meroney RN. Fires in porous media: natural and urban canopies. in Gayev YA, Hunt JCR. (Eds.) *Flow and Transport Processes with Complex Obstructions.* Springer, 2007, Chapter 8, pp. 271-310

[12]   Battaglia F, McGrattan KB, Rehm RG, Baum HR. Simulating fire whirls. *Combust. Theor. Model.*, 2000; 4: 123-138.

[13]   Klimenko AY, Williams FA. On the flame length in firewhirls with strong vorticity. *Combust. Flame*, 2013; 160: 335-339.

[14]   Wang P, Liu N, Hartl K, Smits A. Measurement of the flow field of fire whirl. *Fire Technol.*, 2016; 52: 236-272.

[15]   Hartl KA, Smits AJ. Scaling of a small scale burner fire whirl. *Combust. Flame*, 2016; 163: 202-208.

[16]   Zhou KB, Liu NA, JS Lozano, Shan YL, Yao B, Satoh K. Effect of flow circulation on combustion dynamics of fire whirl. *Proc. Combust. Inst.,* 2013; 34: 2617-2624.

[17]   Lei J, Liu NA, Lozano JS, Zhang L, Deng Z, Satoh K. Experimental research on flame revolution and precession of fire whirls. *Proc. Combust. Inst.,* 2013; 34: 2607-2615.

[18]   Lei J, Li N, Zhang L, Satoh K. Temperature, velocity and air entrainment of fire whirl plume: A comprehensive experimental investigation. *Combust. Flame,* 2015; 162: 745-758.

[19]   Satoh K. Numerical study and experiments of fire whirl. *Proc. 7th Int. Conf., Interflam'96*, 1996, pp. 393-402.

[20]   Zhou R. Applications of the equivalent gap fraction criterion method for fire whirl risk evaluation and prevention in a real fire disaster. *Fire Technol.,* 2014; 50: 143-159.

[21]   Dobashi R, Okura T. Experimental study on flame height and radiant heat of fire whirls. *Fire Technol.,* 2016; 52: 1069-1080.

[22]   Chow WK, Han SS. Experimental investigation on setting internal fire whirls in a vertical shaft. *J. Fire Sci.*, 2009; 27(6): 529-543.

[23] Chow WK. A study on relationship between burning rate and flame height of internal fire whirls in a vertical shaft model. *J. Fire Sci.*, 2013; 32(1): 72-83.

[24] Chow WK, He Z, Gao Y. Internal fire whirls induced by pool fire in a vertical shaft. *Proc. ASME/JSME 2011 8th Thermal Engineering Joint Conference*, 2011, pp. 1-6.

[25] Chow WK, He Z, Gao Y. Internal fire whirls in a vertical shaft. *J. Fire Sci.* 2011; 29(1): 71-92.

[26] GW Zou, Chow WK. Generation of an internal fire whirl in an open roof vertical shaft model with a single corner gap. *J. Fire Sci.*, 2015; 33(3): 35-42.

[27] Zou GW, Hung HY, Chow WK. A study of correlation between flame height and gap width of an internal fire whirl in a vertical shaft with a single corner gap. *Indoor Built Environ.*, Article first published online: September 6, 2017.

[28] Burgess D, Strasser A, Grumer J. Division of fuel chemistry. *Sym. Fire Control Research*, Chicago, Illinois, 1961, pp. 177-192.

[29] Babrauskas V. Estimating large pool fire burning rates. *Fire Technol.*, 1983; 19(4): 251-261.

[30] Rew PJ, Hulbert WG, Deaves DM. Modeling of thermal radiation from external hydrocarbon pool fires. *Process Saf. Environ. Protect.*, 1997; 75(2): 81-89.

[31] Mangialavori G, Rubino F. Experimental tests on large-scale hydrocarbon pool fires. *7th Int. Sym. Loss Prevention and Safety Promotion in Process Ind.*, Taormina, Italy, 1992; vol. 83, pp. 1-11.

[32] Chatris JM, Quintela J, Folch J, Planas E. Experimental study of burning rate in hydrocarbon pool fires. *Combustion Flame*, 2011; 126(1): 1373-1383.

[33] Gasoline Volatility Information. Michigan Department of Agriculture and Rural Development, Laboratory Division/ Motor Fuels Quality, 26 June 2015. https://www.michigan.gov/documents/mda/Gasoline_Volatility_Information_-_endpoint_195239_7.pdf (Accessed 10 September 2018)

[34] Drysdale D. *An Introduction to Fire Dynamics*, 3rd edition, Chichester, England : Wiley, 2011, pp. 188-190.

[35] Shang D. *Free Convection Film Flows and Heat Transfer*. Berlin: Springer; 2006.

[36] Rohsenow WM, Hartnett JD, Ganic EN. *Handbook of Heat Transfer Applications.* New York: McGraw-Hill; 1985.

[37] McCaffrey BJ. Purely buoyant diffusion flames: some experimental results. NBSIR 79-1910, National Bureau of Standards, Gaithersburg, Maryland, 1979, pp. 10-16.

[38] Heskestad G. Engineering relations for fire plumes. *Fire Saf. J.*, 1984; 7(1): 25-32.

[39] Hasemi Y, Tokunaga T. Flame geometry effects on the buoyant plumes from turbulent diffusion flames. *Fire Science and Technology*, 1984; 4(1): 15-26.

FAM_SSLiIFW16A-2o

List of Tables

List of Figures

Table 1. Two sets of experiments

	Label	Gap width(m)	Pool diameter(m)	Fuel volume(L)
Experiment 1	SW 1	0.013	0.46	3
	SW 2	0.055	0.46	3
	SW 3	0.11	0.46	3
	SW 4	0.22	0.46	3
	SW 5	0.33	0.46	3
	SW 6	0.44	0.46	3
	SW 7	0.66	0.46	3
	SW 8	0.88	0.46	3
Experiment 2	SW-S	0.33	0.2	1.25
	SW-M	0.33	0.26	2.12
	SW-L	0.33	0.46	6.65

Table 2. Results of tests: Experiment 1

Exp. 1	SW-1	SW-2	SW-3	SW-4	SW-5(SW-L)	SW-6	SW-7	SW-8	SW-S	SW-M
Gap width	0.013 m	0.055 m	0.11 m	0.22 m	0.33 m	0.44 m	0.66 m	0.88 m	0.33 m	0.33 m
Fire whirl situation	No fire whirl	Flame was higher, no fire whirl	Unstable fire whirl, leapt seriously	Strong fire whirl, leapt slightly	Strong, stable fire whirl	Strong, stable fire whirl	Strong fire whirl, leapt slightly	Intermit tent fire whirl	Strong, stable fire whirl	Strong, stable fire whirl
Burn time	420 s	403 s	284 s	233 s	202（335s）	193 s	203 s	334 s	338 s	328 s
Maximum flame height	1.5 m	1.8 m	3.1 m	3.3 m	3.6 m	3.6 m	3.4 m	3.3 m	1.81 m	2.25 m
Snapshots of flame										

Table 3. Different values of m_∞ given by some researchers about gasoline pool fire

	m_∞ (kg/m^2 · s)
Burgess et al.[28]	0.075
Babrauskas[29]	0.055
Rew et al.[30]	0.067
Mangialavori & Rubino[31]	0.065
Chatris et al.[32]	0.077
This work	0.096

Table 4. Parameters compiled in Experiment 2

Dimensionless gap width	Exp. No.	D_f / m	m/kg	t/s	Q / kW	q^*	L_f / m	X
0.16	SW-S	0.2	0.875	338	88.2	3.94	1.81	5.34
0.16	SW-M	0.26	1.484	328	171.9	3.98	2.25	4.98
0.16	SW-L	0.46	4.665	335	434.5	2.42	3.6	4.89

M10 (C10)
M9 (C9)
M8 (C8)
M7 (C7)
M6 (C6)
M5 (C5)
M4 (C4)
M3 (C3)
M2 (C2)
M1 (C1)

Spacing of 0.9m

D_f=0.46m

Side view of thermocouple trees M and C

0.35m C
0.35m
M
Oil tank

Top view of Thermocouple trees M and C

T22-T11
Spacing of 0.15m

T11-T1
Spacing of 0.1m

SW-S D=0.2m
SW-M D=0.26m
SW-L D=0.46m

Thermocouple tree T
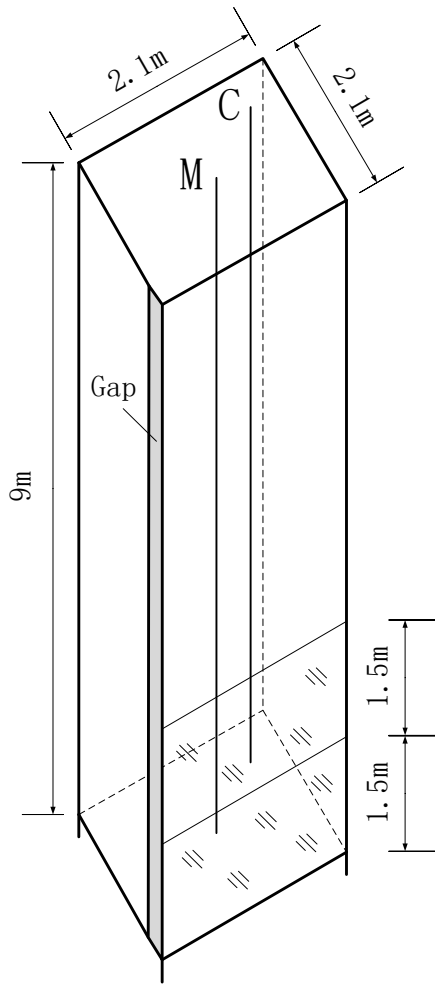
(a) Schematic diagram
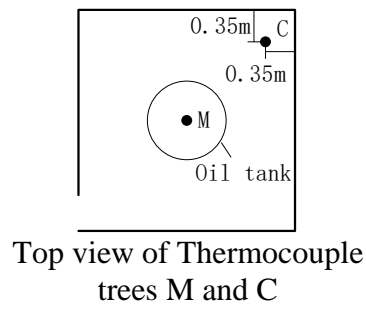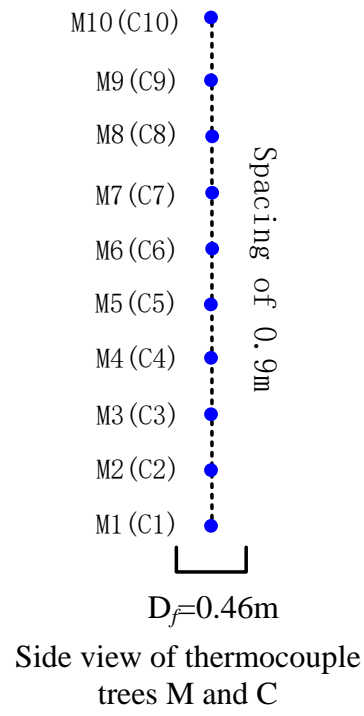
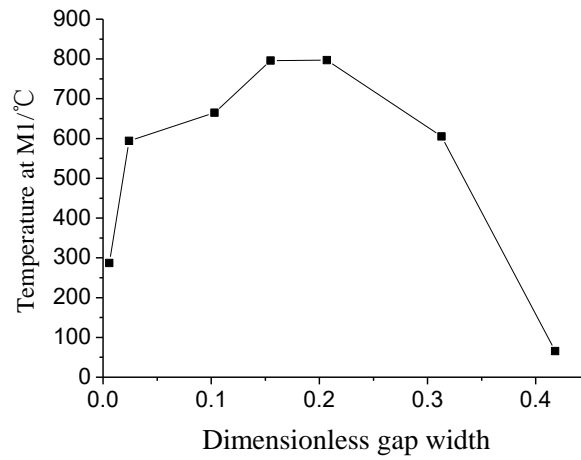(b) Experiment 1
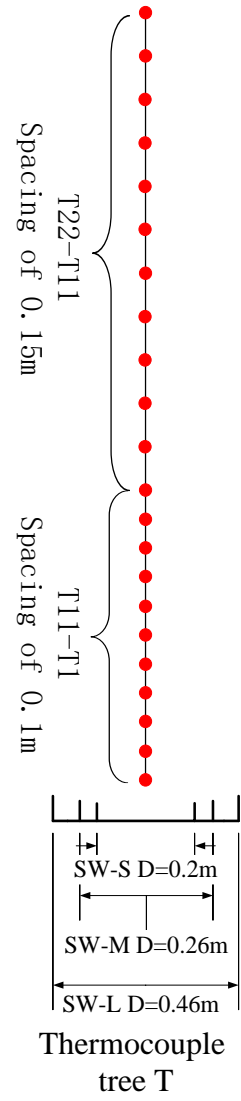
(c) Experiment 2

Fig. 1: Experimental setup
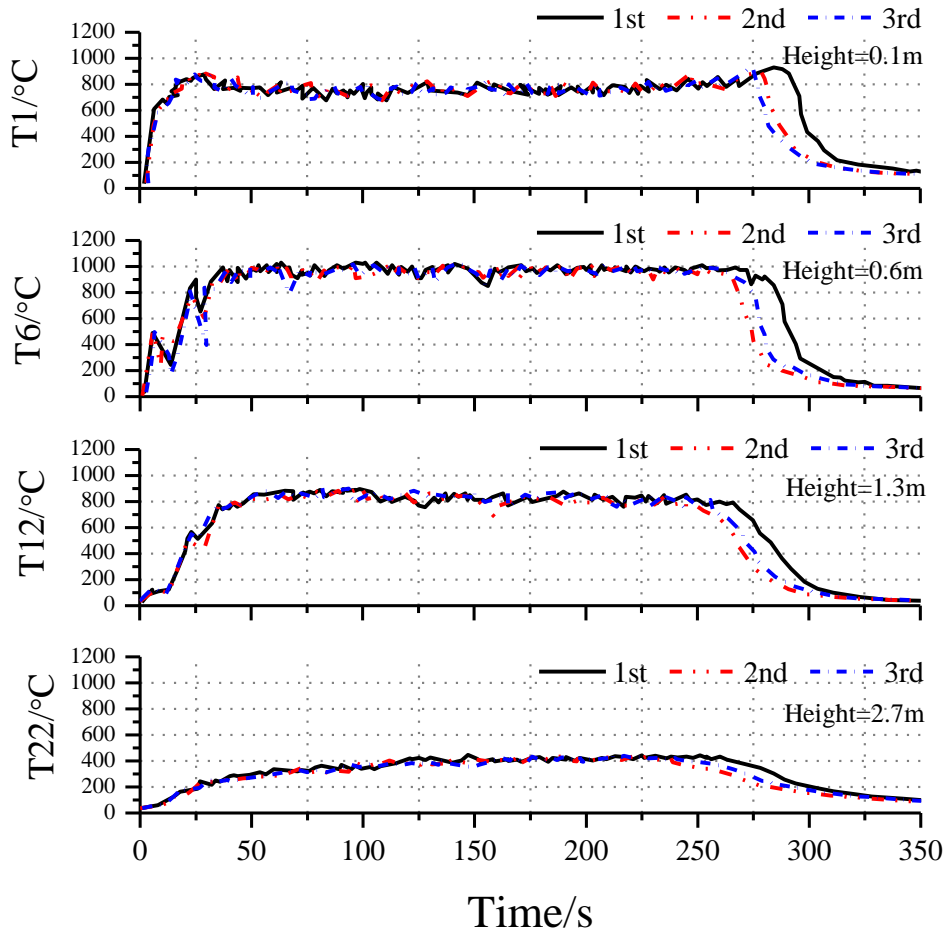
Fig. 2. Temperatures at different heights at central axis
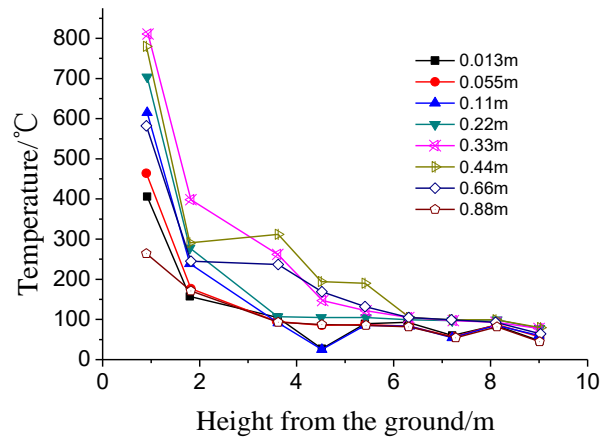
(a) Temperature at thermocouple tree M
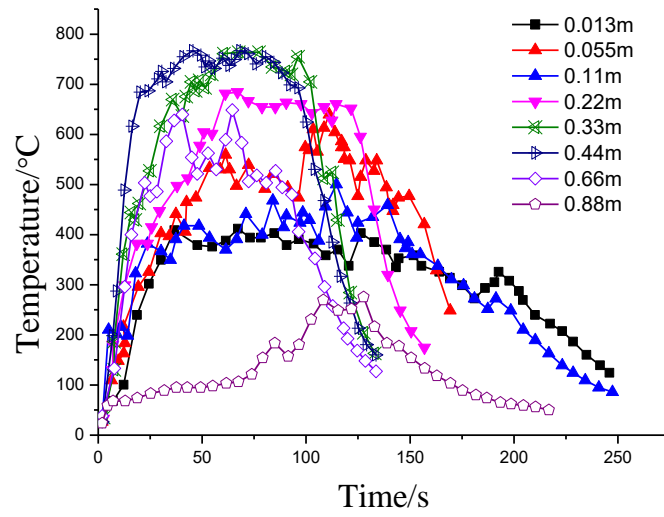
(b) Transit temperature at M1

(c) Average temperature at M1 for a stable IFW

Fig. 3: Variation of temperatures with gap width for Experiment 1
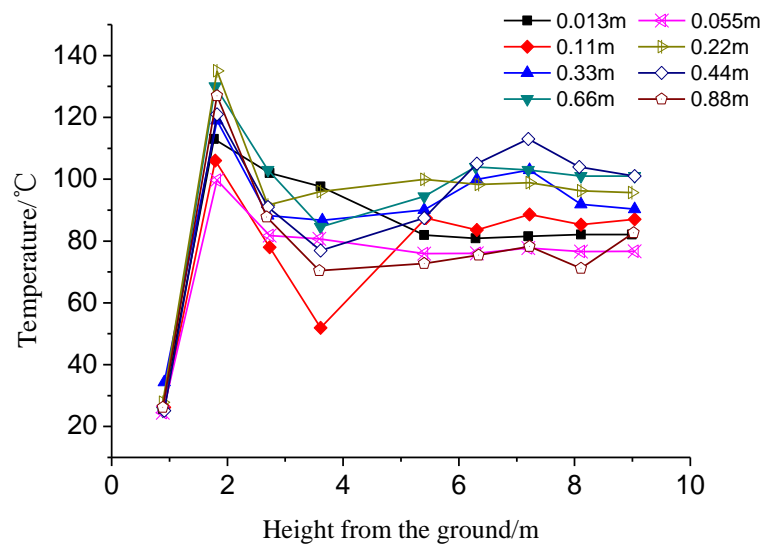
Fig. 4. Variation of temperatures at thermocouple tree C at corner for Experiment 1
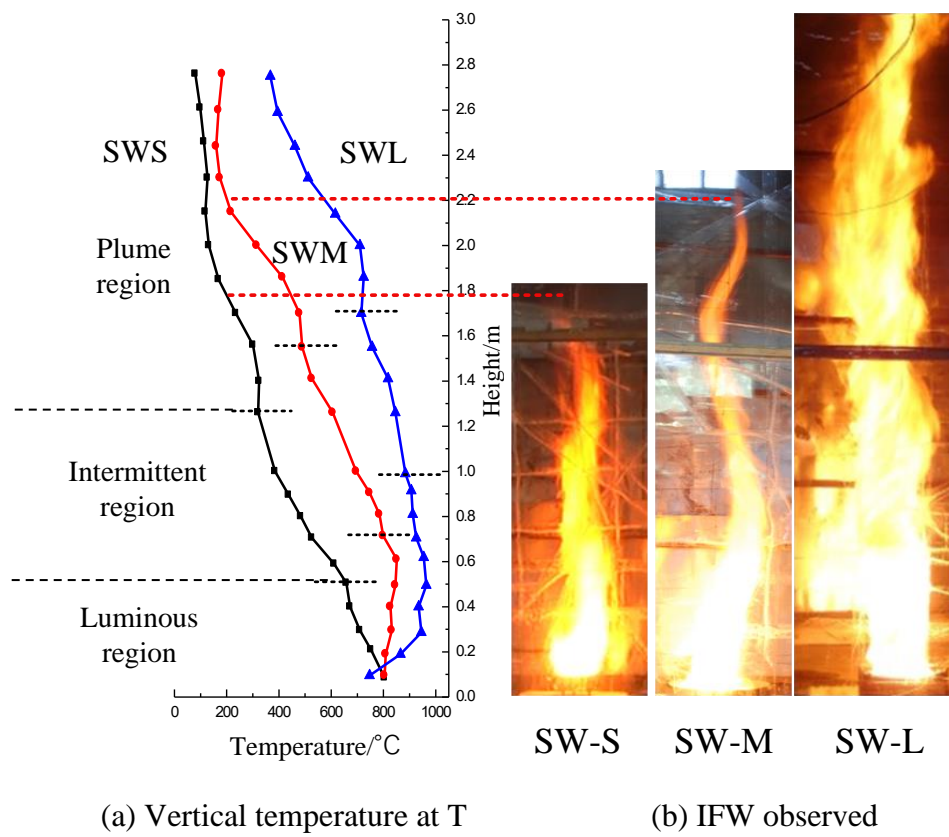

(a) Vertical temperature at T   (b) IFW observed

Fig. 5. Flame height and center line temperature for Experiment 2
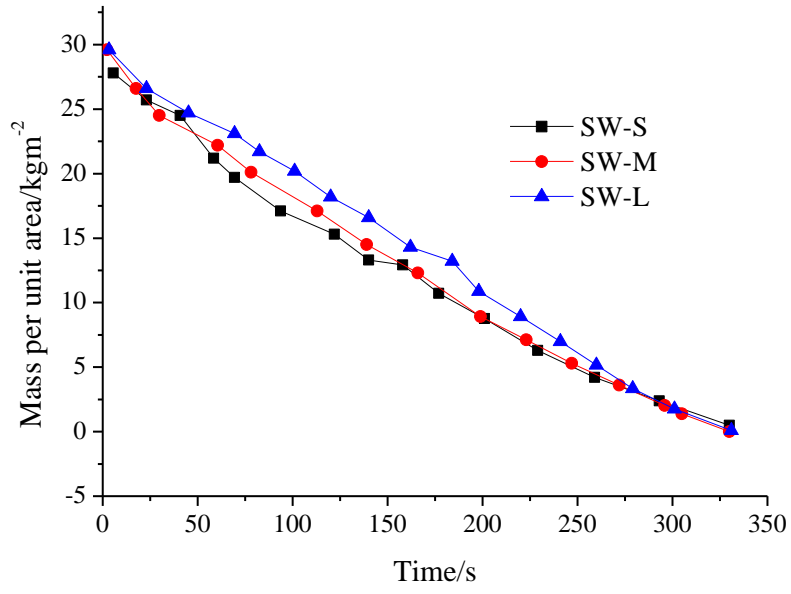
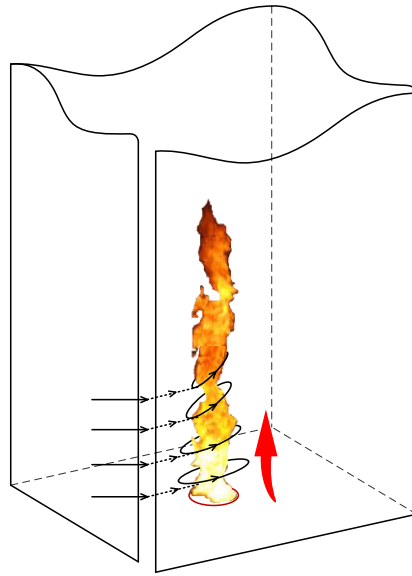Fig. 6. Variation of mass of fuel per unit area with time

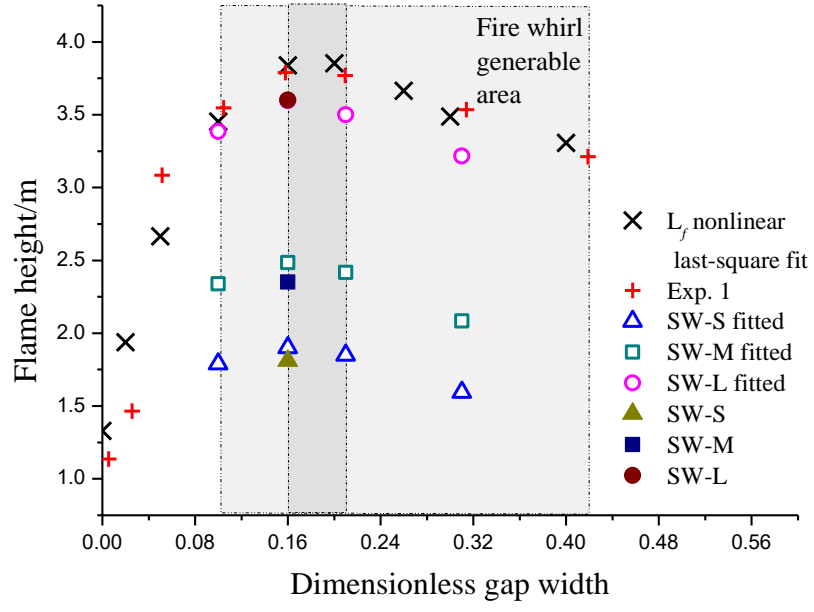Fig. 7. Schematic diagram of axial and tangential velocity
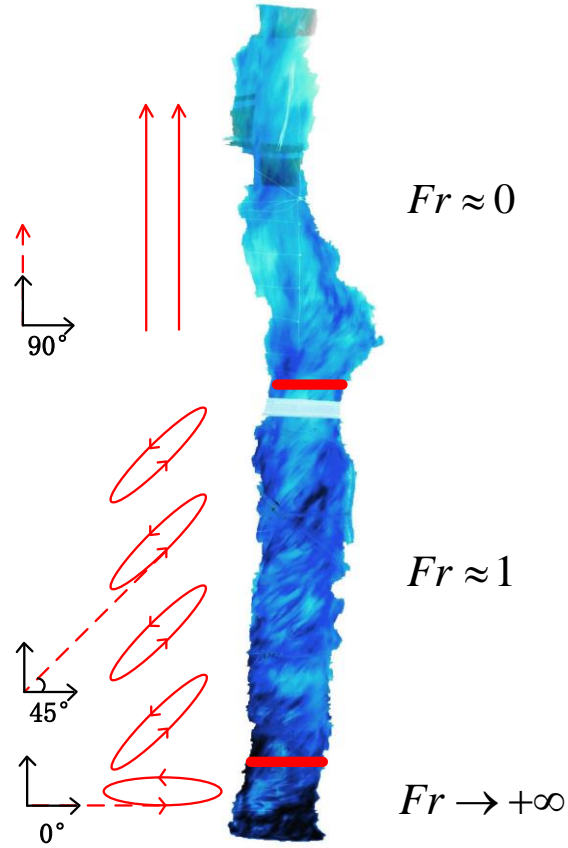
Fig. 8. Dependence of flame height on gap width

Fig. 9. Schematic diagram showing change of *Fr* along the flame